Coupled Ocean–Atmosphere Feedback in the Southern Annular Mode

ALEXANDER SEN GUPTA AND MATTHEW H. ENGLAND

Climate and Environmental Dynamics Laboratory, School of Mathematics, University of New South Wales, Sydney, New South Wales, Australia

(Manuscript received 3 August 2006, in final form 14 November 2006)

ABSTRACT

Previous studies have demonstrated that while the Southern Annular Mode (SAM) is an intrinsic feature of the atmosphere, it projects strongly onto the ocean and sea ice properties and circulation. This study investigates the extent of "back interaction" whereby these oceanic SAM anomalies feed back to the atmosphere. A comparison between atmosphere-only and full coupled climate models demonstrates that air–sea interactions in the coupled system act to increase the persistence of the SAM in the atmosphere. To identify the nature of feedback from the ocean to the atmosphere, ensemble experiments are carried out in both atmosphere-only and full coupled models whereby a continuous SAM-like sea surface temperature (SST) anomaly is imposed. Both coupled and uncoupled experiments show a direct thermal response that affects the lower-tropospheric temperature and surface meridional winds. An indirect upper troposphere–wide response is also seen whose characteristics are sensitive to the coupling. For the uncoupled experiment a negative-phase SAM SST perturbation produces an indirect atmospheric response that projects strongly onto the SAM. A positive-phase anomaly, however, shows little robust response away from the local heating at the surface. The coupled experiments, however, do show linearity with respect to the sign of the anomaly. However, the response is considerably weaker than the uncoupled case and the projection of the response onto the SAM mode is poorer. Nonetheless the authors find a clear persistence of the SAM at interseasonal time scales that relies on air–sea coupling and cannot be reproduced in unforced atmosphere-only experiments. This demonstrates that the ocean plays a role in modulating the Southern Annular Mode at these time scales.

1. Introduction

There is a growing effort to predict the future state of the intrinsically chaotic atmosphere in terms of more predictable, slowly varying, external forcing. Candidates for this include seasonal–interannual changes in the mean state of the ocean and gradual changes in radiative forcing due to an enhanced greenhouse effect or altered atmospheric chemistry. For tropical variability, most notably the Southern Oscillation, there is a clear connection between changes in sea surface temperatures (SST) and the overlying atmospheric circulation. As the atmosphere is readily overturned in the Tropics, surface anomalies are effectively transmitted through the atmosphere. This is not the case at higher latitudes where the atmosphere is more stably stratified. Nevertheless there is a growing consensus that there does exist a significant, albeit weak, influence of the ocean on the atmospheric circulation outside of the Tropics. Much of the research on the feedback from the ocean to the atmosphere in the extratropics has focused on the Northern Hemisphere and in particular on the Northern Annular Mode.

Magnusdottir et al. (2004), for instance, use long integrations of an atmospheric general circulation model (AGCM) forced with a control climatology with a superimposed perturbation based on an exaggerated trend in North Atlantic SST or sea ice extent. They find a weak positive feedback associated with the SST perturbation, however only a small fraction of the full North Atlantic Oscillation (NAO) trend is explained. The sea ice perturbation produces a considerably stronger response, however the resultant trend is of the wrong polarity, indicating a significant negative feedback. Using an SST perturbation of reversed polarity, significant nonlinearities in the response with respect to the sign of the perturbation are seen. Further analysis by Deser et al. (2004) shows that the response can be

Corresponding author address: Alex Sen Gupta, Climate and Environmental Dynamics Laboratory (CEDL), School of Mathematics, University of New South Wales, Sydney, NSW, Australia.
E-mail: a.sengupta@unsw.edu.au

DOI: 10.1175/JCLI4200.1

split into an indirect component that projects onto the leading mode of natural variability—the NAO—and a residual, direct, component that represents the local thermal response to the SST anomaly resulting in a modified surface baroclinicity. A number of studies also find additive nonlinearity when combining perturbations from different regions (e.g., Sutton et al. 2001; Peng et al. 2002; Robinson et al. 2003). For instance, the atmospheric response to an NAO-like SST forcing is significantly different from the additive response to the separate subtropical and extratropical part of the same SST pattern. This is despite the fact that the resulting anomalous heating and zonal flow exhibit additive linearity (Robinson et al. 2003).

These results are generally consistent with findings of earlier Northern Hemisphere studies as reviewed by Kushnir et al. (2002). They find that modeling studies generally show a significant large-scale extratropical SST influence on atmospheric variability although the responses are relatively weak compared to the magnitude of the intrinsic atmospheric variability. The nonlinear interaction between transient eddies and the atmospheric mean flow that excite and maintain the dominant modes of variability is also implicated in any response to SST anomalies. As a result, a large part of any response often projects onto these dominant atmospheric modes. The direct linear response is primarily confined to a local, near-surface thermal response.

There is also evidence that the dominant mode of Southern Hemisphere variability—the Southern Annular Modes (SAMs)—exhibits a certain degree of "back interaction" from the ocean to the atmosphere. The SAM represents a zonally symmetric shift in the strength and position of the subtropical jet, with a positive SAM phase corresponding to a stronger more poleward contracted jet and a negative phase corresponding to a weaker lower-latitude jet. The SAM shows significant signatures in oceanic and sea ice properties and circulation (Hall and Visbeck 2002; Holland et al. 2005; Sen Gupta and England 2006). Watterson (2001) examined SAM behavior in multicentury runs of an atmospheric model forced by a monthly climatology, coupled to a slab ocean and coupled to a full ocean general circulation model (OGCM). With an interactive ocean, Watterson (2001) finds a feedback from the ocean to the atmosphere that on short time scales affects lower-tropospheric temperatures but on interannual time scales has a significant effect on tropospheric zonal winds. On interdecadal time scales the ocean coupling explains a large fraction of the variability. Zhou and Yu (2004) used the National Center for Atmospheric Research (NCAR) Community Atmosphere Model version 2 (CAM2) AGCM to see if, by prescribing historical SST, the model shows any skill in reproducing the observed SAM signal. They show some reproducibility particularly in the austral summer. However, they ascribe much of the model's success to variations in tropical Pacific SST and the resulting teleconnections to high latitudes rather than to local ocean feedbacks at the Southern Hemisphere midlatitudes.

Sen Gupta and England (2006) use output from a 200-yr present-day control run of the NCAR Community Climate System Model version 2 (CCSM2; the forerunner to the model used in this study) to investigate the response of the ocean and sea ice to SAM variability. A heat budget analysis demonstrates that the SAM is associated with anomalous oceanic meridional heat advection (via Ekman transport), surface heat fluxes, and changes in mixed layer depth, which act in phase to imprint a strong circumpolar SAM signature onto SST. Lagged correlations show that although the SAM is mainly controlled by internal atmospheric mechanisms, the thermal inertia of the ocean reimprints the SAM signature back to surface air temperatures (SATs) on time scales longer than the initial atmospheric signal. SAM-driven sea ice anomalies also persist for many months as a result of an albedo feedback mechanism. In the present study, we further investigate the role of the ocean–atmosphere interaction to see if there is any significant response beyond the direct thermal link to the lower troposphere. For this purpose, a series of uncoupled and coupled experiments are performed using the NCAR CCSM3 (version 3) in which SAM-like perturbations are added to the ocean. The intrinsically noisy atmospheric circulation requires the use of large ensembles to identify statistically robust responses, particularly when the back interaction in the extratropics is thought to be weak (Kushnir et al. 2002; Watterson 2001). To our knowledge this is the first attempt to apply to the SAM the same perturbation techniques used to investigate air–sea coupling in the NAO. In addition, while a number of studies use comparisons between coupled and uncoupled GCMs to investigate the role of coupling in ocean–atmosphere interaction (e.g., Kushnir et al. 2002; Watterson 2001), we attempt to directly excite a SAM response in the atmosphere through the application of annular wind perturbations within a full coupled climate system.

The remainder of this paper is divided as follows. In section 2 we briefly introduce the CCSM3 climate model and describe the way in which perturbations were applied and the ensembles implemented within the coupled and uncoupled systems. In section 3 we compare natural variability runs for a number of coupled and uncoupled runs and describe results from

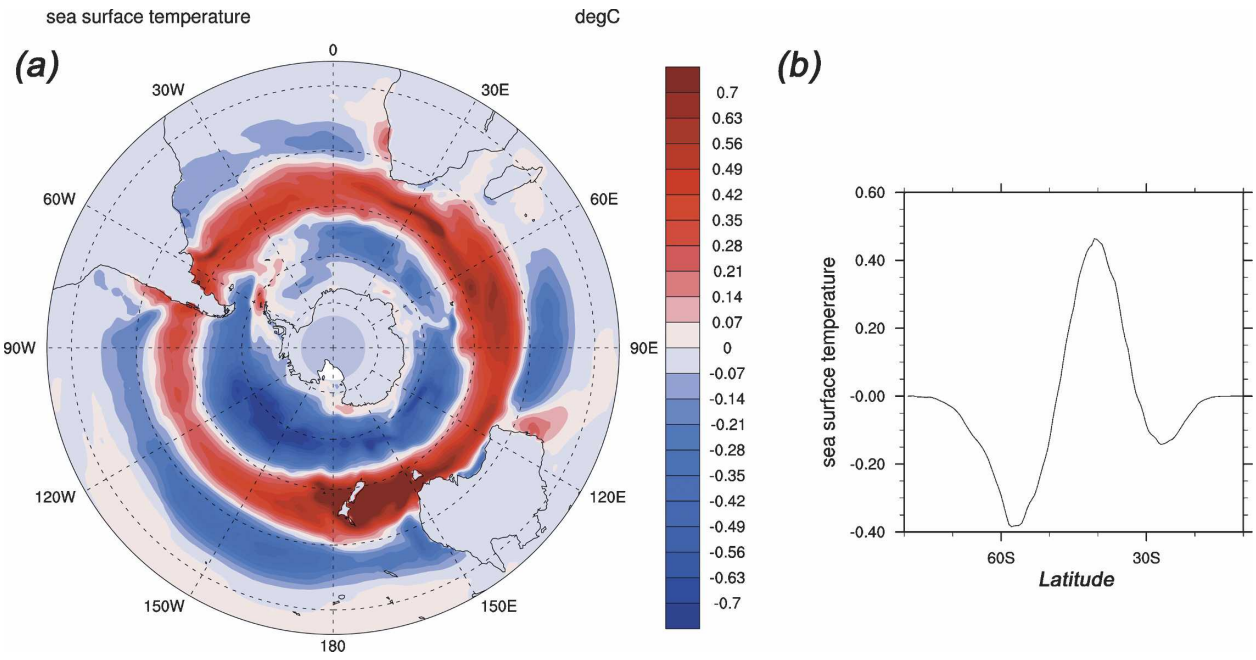

FIG. 1. (a) Lateral and (b) zonally averaged SST anomaly added to the "natural variability" control climatology for the positive perturbation experiments (anomaly inverted for negative perturbation experiments). This is equivalent to 3 times the SST regression onto the PD experiment SAM index.

the uncoupled (section 3a) and coupled (section 3b) ensemble perturbation experiments. Finally, a summary and conclusions are presented in section 4.

2. Methodology

Ocean–atmosphere coupling associated with the SAM is investigated in the NCAR Community Climate System Model version 3.0. This is a coupled climate model with interactive components representing the atmosphere (CAM3; Collins et al. 2006b), the ocean (Parallel Ocean Program; POP; Danabasoglu et al. 2006), sea ice (Community Sea Ice Model; CSIM; Briegleb et al. 2004), and the land surface (Community Land Model; Oleson et al. 2004). All experiments were conducted with the atmosphere and land surface at a T42 horizontal resolution (approximately 2.8° × 2.8°) with 26 hybrid sigma/pressure vertical levels in the atmosphere. The ocean and sea ice components have an approximate horizontal resolution of 1° with 40 vertical levels in the ocean. The coupled model is able to run without the need for any flux adjustments, maintaining a steady present-day climate state that reproduces the main features of the observed system. A detailed account of the coupled model is presented by Collins et al. (2006a) and in the associated special issue of the *Journal of Climate*. The last 200 yr of a fully coupled 1000-yr control run using perpetual 1990 conditions are used here as a base simulation [hereafter present day (PD)]. Both coupled and uncoupled ensemble experiments have been initialized from near the end of this base experiment. Additional runs, including 200 yr from a 700-yr 1870 control run plus a set of 50-yr "atmosphere-only" and "atmosphere- and land-only" runs with prescribed SST and sea ice, were also used for coupled/uncoupled experiment comparisons.

An ensemble of runs was carried out with only the atmosphere active to investigate how SAM-like anomalies in SST might feedback to the atmosphere. In these experiments all other components were replaced by prescribed monthly climatologies of the necessary forcing variables based on a long-term climatology of the PD run. Onto the prescribed SST climatology a constant SST anomaly was imposed based on the regression pattern of monthly SST anomalies onto the SAM index (from the PD run). The SST perturbation corresponds to a three standard deviation SAM anomaly (Fig. 1). The large magnitude makes it easier to extract a robust response from the noisy atmospheric signal. Forty positive and forty negative ensemble experiments were conducted. Five ensemble members were started with the perturbations beginning a day apart between 1 January and 5 January. In addition, 8 different starting years were used between 5 and 10 yr apart (giving the total of 40 ensemble members). Each ensemble member was integrated for 3 months. Experiments were lim-

ited here to a single season in order to exclude seasonal factors from influencing the ensemble set. The austral summer period was chosen, as the SAM index shows enhanced persistence at this time of year. This seasonality is further discussed below.

An additional set of perturbation experiments was carried out using the full coupled model. Here a time-varying wind stress anomaly, based on a linear interpolation between twelve monthly perturbation patterns, was added in such a way that only the ocean was directly affected by the perturbation (via an altered Ekman transport). The atmosphere is only indirectly affected by the resulting changes in heat fluxes due to the modified SST distribution. The monthly wind stress anomalies were based on the regression of wind stress onto the SAM index from the PD integration. A perturbation corresponding to a two standard deviation SAM was used in this case. This produced an SST anomaly of similar magnitude (i.e., 3 standard deviation SAM) to that prescribed in the uncoupled ensemble experiment. This is possible as a continuous wind stress is applied that causes SST to gradually build up across the sharp temperature fronts of the Southern Ocean until a balance is reached with the surface heat fluxes. Twenty positive and twenty negative ensemble experiments were carried out, each starting on 1 January of successive years. Each ensemble member was integrated for 6 months.

Comparisons are made between ensemble means of the positive (P), negative (N), and control (C) runs. By comparing positive and negative ensemble means we have the potential to effectively double the amplitude of the perturbation (assuming that there is a degree of linearity with respect to the sign of the perturbation). For the uncoupled experiments a 50-yr unperturbed atmosphere-only run was used to provide control ensemble members. A standard *t* test is used to assess the statistical significance of the differences between the means. Note that both these configurations of ensemble experiments—whether coupled or uncoupled—are used to explore the potential for ocean–atmosphere feedback in the SAM.

3. Results

Figure 2 shows a comparison between the simulated (PD experiment) and observed European Centre for Medium-Range Weather Forecasts (ECMWF; Gibson et al. 1996) sea level pressure (SLP) regression onto the SAM index. Following Sen Gupta and England (2006), the SAM indices were calculated as the standardized principal component associated with the dominant empirical orthogonal functions (EOFs) of monthly SLP anomalies south of 20°S. In the simulation this mode accounts for ~35% of the SLP variability as opposed to ~28% in the observations. The patterns show a strong similarity in their zonal structure, with coincident regions of maximum high pressure between 45° and 50°S and minimum low pressure between 75° and 80°S. Both patterns show an enhanced low pressure region in the central/eastern Pacific, although this is more prominent in the observations. Enhanced high pressure regions are also evident to the east of New Zealand and in the Indian Ocean Basin. The latter anomaly is again more prominent in the observations. In the zonal average the simulated SAM pattern has a larger magnitude particularly for the midlatitude maximum (Fig. 2c). Surprisingly, this is at odds with the higher-resolution transient twentieth-century ensemble runs of the CCSM3, which show the simulated SAM response to be considerably weaker than that of the National Centers for Environmental Prediction (NCEP)–NCAR reanalysis (Raphael and Holland 2006). Power spectra of the SAM indices (Figs. 2d,e) both show a reddening at longer time scales. However, this reddening is significantly stronger in the simulation. This may be a function of the short observational time series used here, which spans only 23 yr to minimize the effect of less reliable years in the climatological records. These results are, however, robust when the observational analysis is extended back to 1960.

Figure 3 shows the power spectrum of the SAM index calculated for a series of full coupled, atmosphere–land and atmosphere-only integrations. To make for a more meaningful comparison, the PD coupled run is only shown for a representative 50-yr segment to match the atmosphere–land and atmosphere-only run lengths (other 50-yr segments show equivalent characteristics). All simulations are consistent with a red noise power spectrum. However, the three runs that lack an interactive ocean and marine cryosphere show a loss of power at interannual time scales. This feature has also been seen in coupled and uncoupled versions of the Commonwealth Scientific and Industrial Research Organisation (CSIRO) climate model (Watterson 2001). Watterson (2001) goes on to show that in a simple model of the oceanic mixed layer thermal response to stochastic atmospheric vacillations, the low-frequency power in the atmospheric variability is only successfully captured by allowing the ocean component to feedback to the atmosphere. Analogous Northern Hemisphere modes of variability have also been shown to be affected by coupled air–sea interactions (Kushnir et al. 2002). An interesting feature of the three uncoupled power spectra is a significant peak at about 6 months. Taken in isolation one would expect around 5% of the spectrum to exceed the 95% confidence level. How-

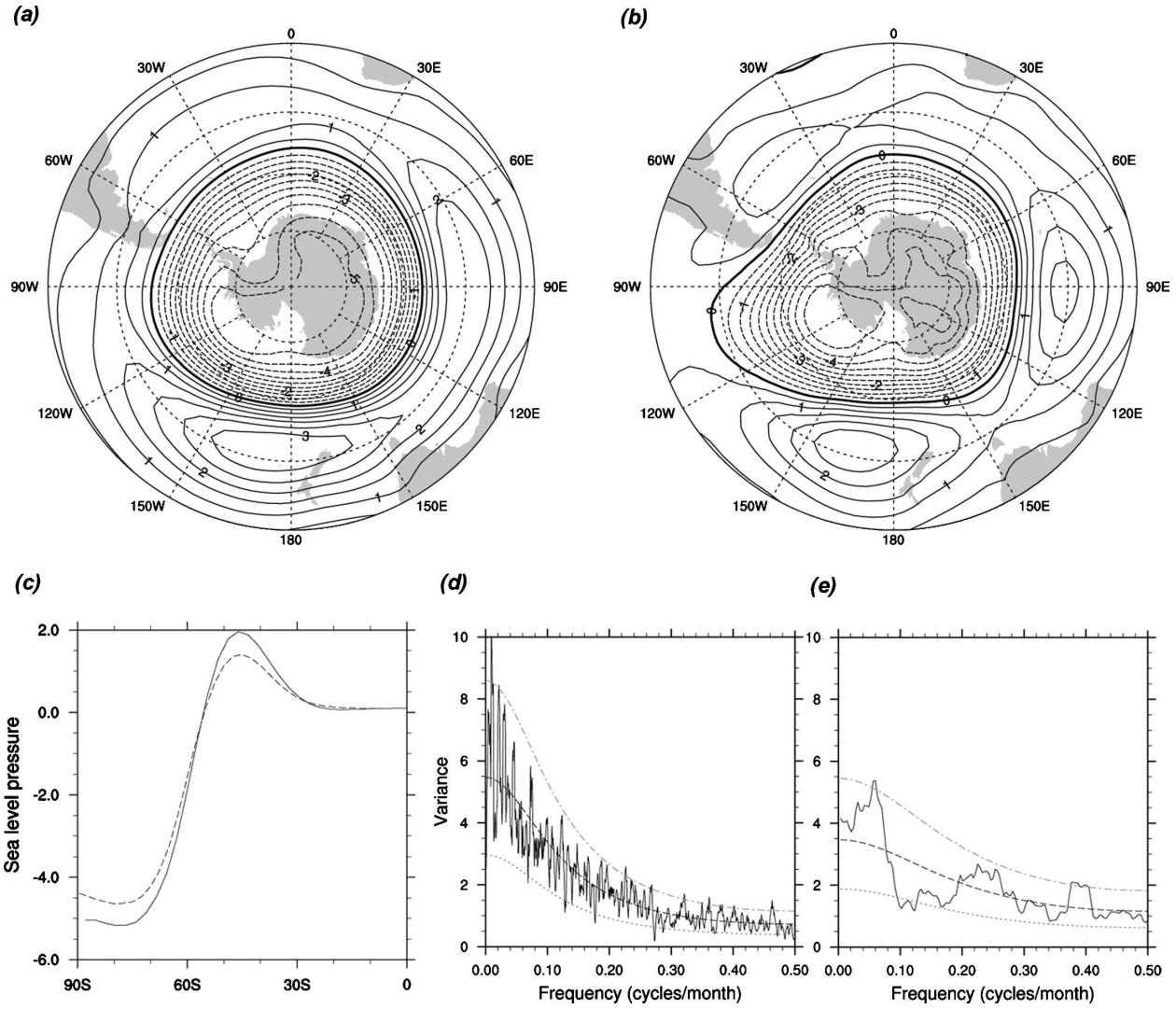

FIG. 2. Regression on SAM index of (a) 200-yr CCSM3 1990 coupled control run, (b) ECMWF (1979–2002), and (c) zonally averaged SLP anomalies (mb). In (c) the solid line is simulation and dotted line is ECMWF regressions. Power spectra are for (d) simulation and (e) observations.

ever, the fact that all three experiments show extra power at this time scale is suggestive of a robust biannual modulation of the SAM index. This is possibly a result of the modulation of the SAM variability by the semiannual oscillation (SAO), which is well represented in CCSM3 (Raphael and Holland 2006). As the simulations are natural variability rather than transient forced runs, it is unlikely that all three simulations would exhibit a long-term modulation that might produce such a peak in the power spectrum. The SAO is a seasonal-scale mode with a similar spatial structure to the SAM but is associated with a biannual modulation of the tropospheric zonal temperature gradient (van Loon 1967). It is unclear why this peak is not also present in the coupled simulations.

Figure 4a shows the lagged autocorrelation for the SAM indices in the uncoupled and coupled experiments described above with the addition of a second 200-yr coupled "preindustrial" experiment. Again there is a notable difference between the experiments *with* and *without* coupling to a dynamic ocean and cryosphere. In the uncoupled integrations there is little persistence of the SAM index beyond about 2 months. This is extended by many months in the case of the coupled system. To verify that this is not just an artifact of the shorter lengths of the uncoupled integrations, the long PD control simulation was split into 4×50 yr sequential segments. Each of these 50-yr segments showed an autocorrelation decay time scale consistently longer (on the order of 4–6 months) than the

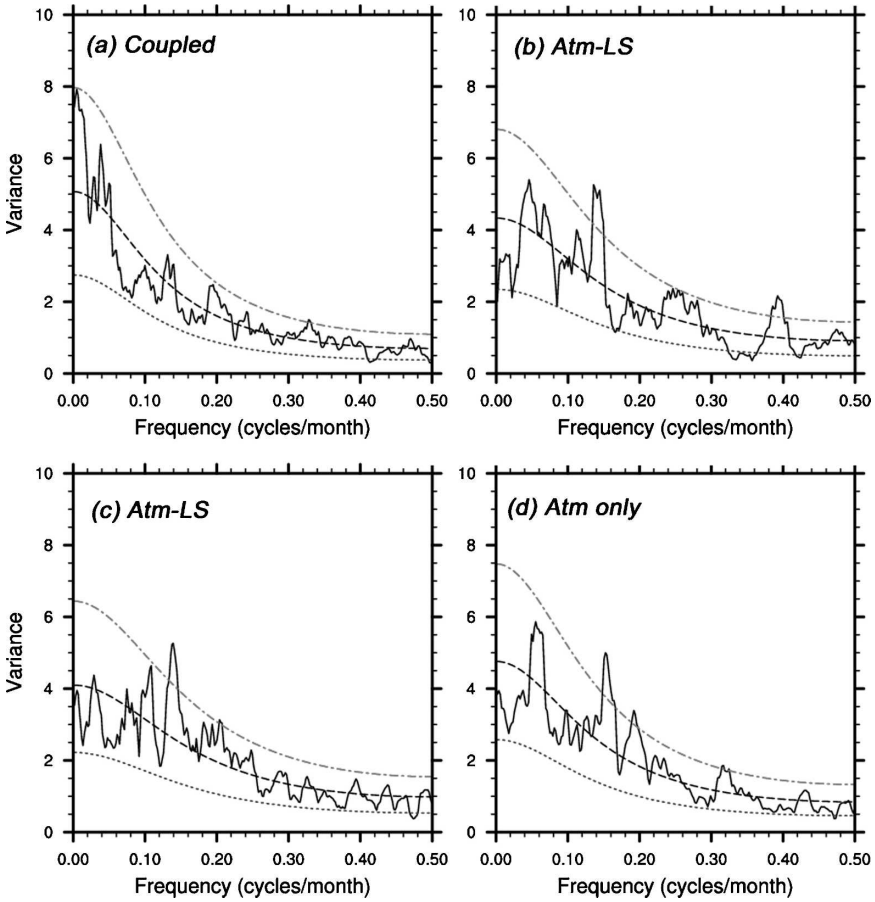

FIG. 3. Power spectra for (a) 50 yr of the fully coupled 1990 control integration, (b) 50-yr integration with atmosphere and land components active (ocean and ice prescribed by observed climatology), (c) similar to (b) but with ocean and ice prescribed by the 1990 control run, and (d) 50-yr integration with only the atmosphere component active (ocean–ice–land prescribed by observed climatology). Dashed lines represent theoretical red noise (Markov) spectrum (with 95% confidence limits) generated using a lag-1 autocorrelation of respective time series.

SAM index in the 50-yr uncoupled integrations (on the order of ~2 months). In a study of the effects of ocean coupling on the SAM, Watterson (2001) also finds, based on 1000-yr integrations of the CSIRO model, enhanced low-frequency power when a coupled ocean is included. His simulations do not show as pronounced an increase, however the longer integration times make the difference significant. Autocorrelations from the Watterson (2001) study are shown in Fig. 4 for comparison. Lagged autocorrelations were also calculated for the PD integration but with certain seasons removed from the SAM index time series (Fig. 4b). This clearly shows a greater persistence in the index with the April–June or July–September seasons removed; that is, the greater persistence is primarily driven by mechanisms occurring in the austral summer. As this corresponds to the time of minimum ice extent, this suggests that it is the coupling with the ocean, rather than with dynamic sea ice, that is of primary importance to any positive feedback into the atmospheric mode of variability. It is possible that seasonality in the SAM variability is also a factor, particularly as the greatest variance in the PD experiment is seen in January. However, variations are relatively small and do not show a smoothly varying seasonality.

a. Uncoupled experiments

As both the atmospheric and oceanic manifestations of the SAM have a high degree of zonal symmetry, we will often only present zonally averaged fields in the following analyses. Figure 1 shows the SST perturbation added to, or subtracted from, the monthly climatology in the uncoupled positive and negative ensemble runs. This pattern is the integrated response of the

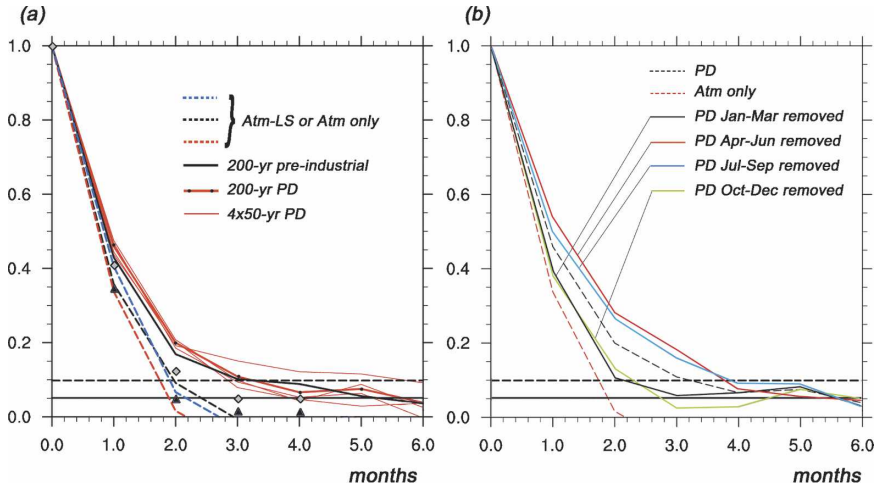

FIG. 4. (a) Autocorrelation of the SAM index for two 200-yr coupled integrations [PD (thick solid red line) and a preindustrial control run (solid black line)] and for the uncoupled prescribed ocean/ice integrations described in Fig. 3. Thin red lines show results for PD time series broken into 4×50 yr sequential subseries. The 95% confidence intervals are also shown (horizontal lines; lower line for coupled 200-yr experiments). Autocorrelation values taken from long integrations of the CSIRO model (Watterson 2001) are shown: gray diamonds are for the coupled model and black triangles are for prescribed SST. (b) Autocorrelations of the SAM index for the coupled PD integration (dashed black line), an atmosphere-only integration (dashed red line), and PD integration with seasons (January–March, April–June, July–September, and October–December) removed from the time series.

ocean to SAM-modified surface heat fluxes (resulting primarily from modified atmospheric temperatures and water content), altered meridional heat flux (driven by the modified zonal wind), and changes to the mixed layer depths (caused by a combination of SST changes and altered wind stresses; Sen Gupta and England 2006). To extract a robust response from an inherently noisy atmosphere, the signal has a magnitude 3 times that of a "normal" (i.e., one standard deviation) monthly SAM anomaly. The ensemble mean response of SLP to the SST perturbation is shown in Fig. 5. Both the difference between positive and negative ensemble means and the difference between positive or negative means from a 50-yr control simulation are shown. The combined SLP response projects strongly onto the SAM pattern, with a node near 60°S, low pressure to the south, and a maximum high pressure anomaly to the north of this latitude band. While there is a nonzero response in the Northern Hemisphere, it is not statistically significant. The comparison of the perturbation responses to the control run (Figs. 5d,e) indicates that there is a significant nonlinearity in the response with respect to the sign of the perturbation. While the negative perturbation experiments indicate a positive feedback (i.e., a negative SAM-like SST pattern is producing a negative SAM-like SLP pattern), the positive perturbation shows practically no robust response. Only at ~60°S is there a small region that is statistically significant (Fig. 5e). This corresponds to the nodal point in the SAM response where variability is small anyway, so little confidence should be attached to this. It should also be noted that even though a three standard deviation SST perturbation was imposed, the negative experiment shows a response that is slightly weaker than a one standard deviation SLP SAM response (cf. red line in Fig. 5c). Similar results are seen for the zonal and meridional wind responses (Fig. 6). Only the negative ensemble experiments show a response that projects significantly onto a negative SAM, with a magnitude similar to a one standard deviation SAM response. The meridional wind response is generally consistent with the surface signature of the zonal response, wherein the boundary layer surface drag deflects the geostrophic zonal wind to give a meridional component to the winds. The anomalous northerly wind to the north of 45°S does, however, appear to be shifted southward compared to the SAM regression. A small statistically significant response region of northerly wind is also seen for the positive experiment near 45°S where the SAM regressed meridional wind shows a region of weak wind anomaly. This is discussed further in the next section. Finally, the temperature response is shown in Fig. 7. Away from the area directly affected by the SST perturbation, the response is consistent with

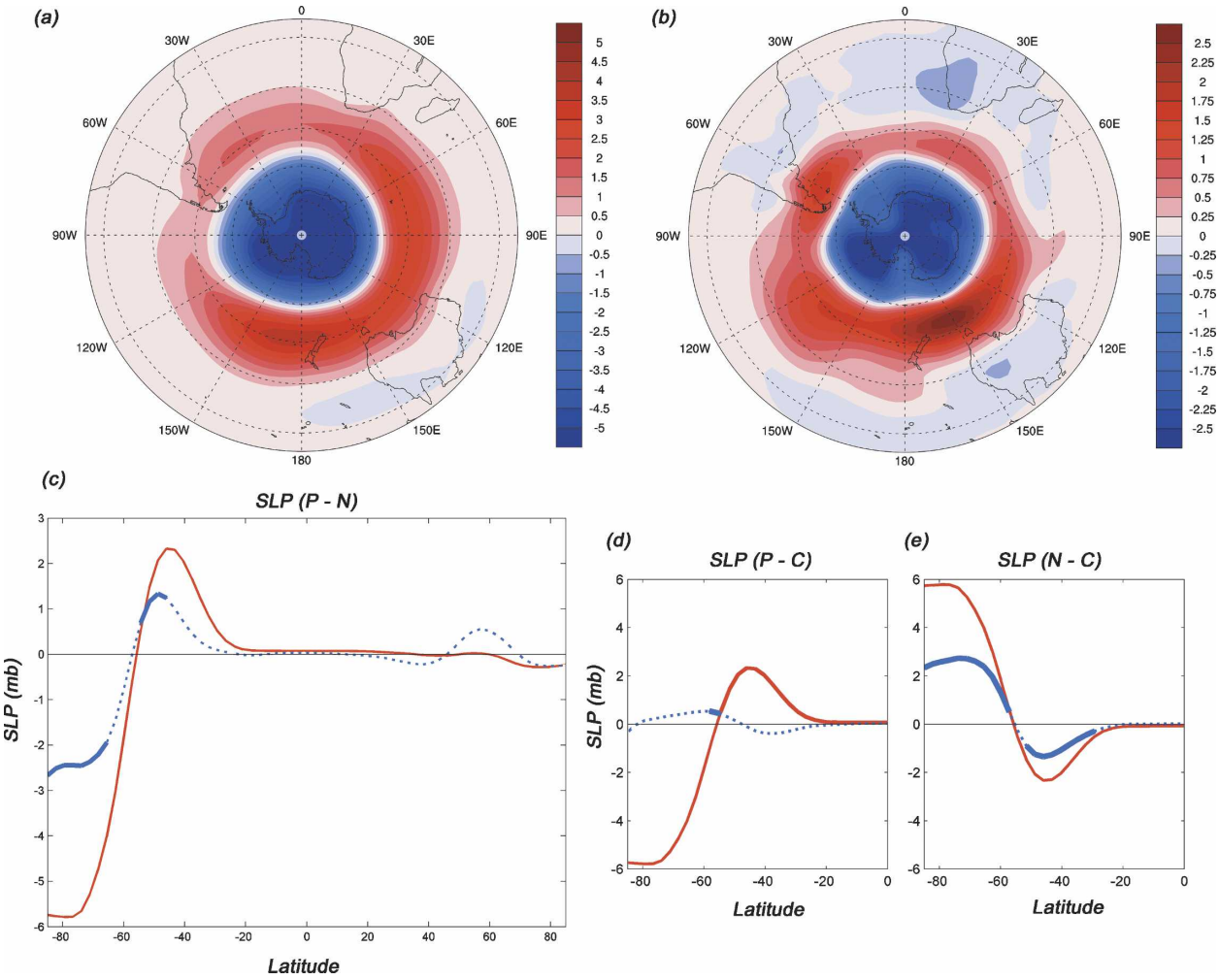

FIG. 5. (a) Regression of SLP (mb) onto the SAM index for atmosphere-only control; (b) difference between the positive and negative experiment ensemble means (P − N) for SLP; (c) zonal averages of SLP regression shown in (a) (red line) and ensemble mean difference shown in (b) (blue line; line is solid where the difference is significant at 95%). (d), (e) Same as in (c) but for P − C and N − C ensemble means.

previous results, namely, a significant positive feedback from the negative experiment and only a weak feedback in the positive experiment. Near the surface, however, extending through to heights of ~1 km, a superimposed temperature anomaly is evident for both the positive and negative experiments that mirrors the surface temperature perturbation in the ocean.

b. *Coupled experiments*

It is conceptually more difficult to add perturbations within a coupled system. Any anomalies that are added outside of the system's boundary conditions (in the coupled case this is only the radiative forcing) will not be physically consistent. Internal perturbations are, however, commonly used in the form of flux adjustments when a coupled model shows a consistent bias and drifts away from a realistic climate, although these adjustments are not used in the CCSM3. Here, we apply a double standard deviation SAM-like wind stress anomaly in such a way that only the ocean dynamics are directly affected (see Figs. 8a,b). This acts, via Ekman transport, to advect the surface layers to the north at high latitudes and to the south at midlatitudes (Fig. 8c). The mostly meridional advection of heat produces a SAM-like SST pattern (Fig. 8d) that builds in magnitude until a balance is achieved through surface heat fluxes and oceanic mixing. The magnitude of the resulting response can be significantly larger than that generated through normal atmospheric variability, as we are imposing a large continuous perturbation that allows the response to gradually build up over time. While wind anomalies in nature also directly affect sur-

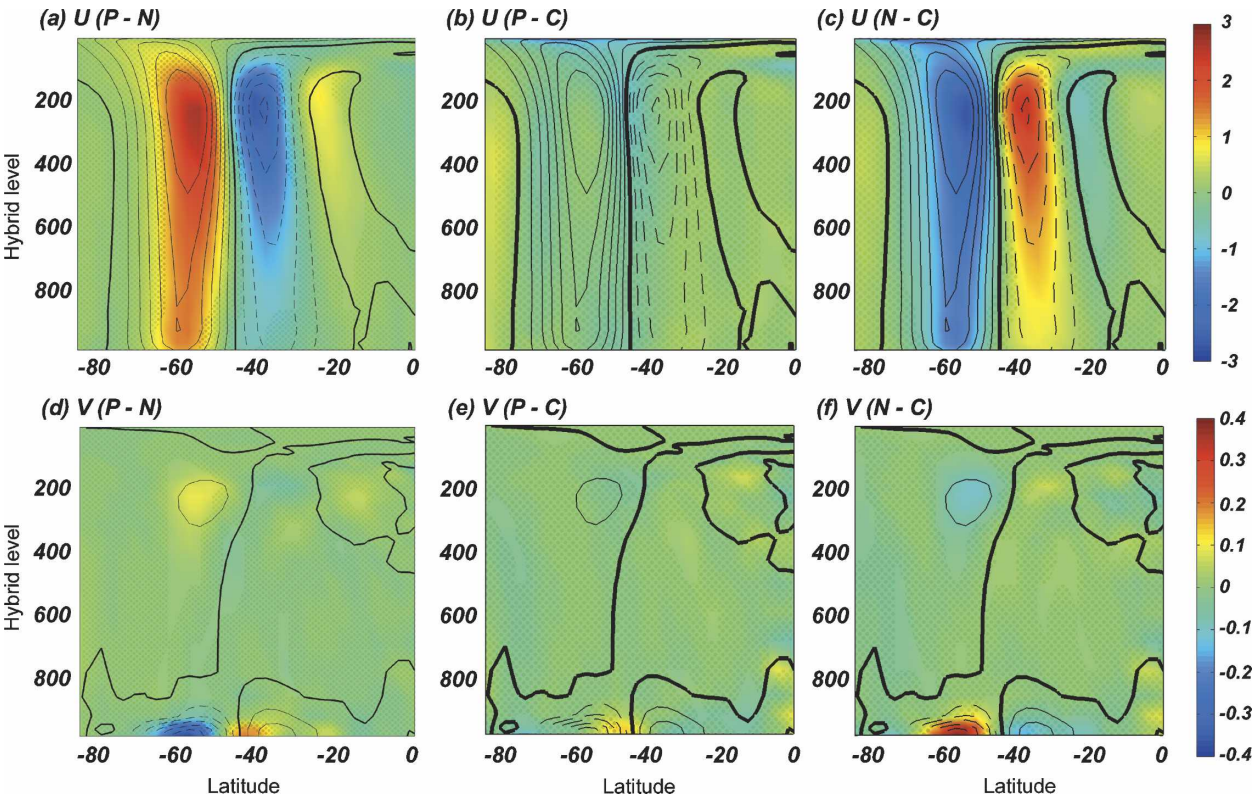

FIG. 6. (a) Difference between positive and negative experiment ensemble means for zonally averaged zonal velocity (filled contours; mottling indicates areas where difference is not significant at 95% level). Black contours show the zonally averaged zonal velocity regressed on the SAM index (solid lines are positive, dashed lines are negative, and thick line at 0; contour interval is 0.5 m s^{-1}). (b), (c) Same as in (a) but for the differences in the P − C and N − C ensemble means. (d)–(f) Same as in (a)–(c) but for the zonally averaged meridional velocity. Regression contour interval (CI) is 0.1 m s^{-1}. All vertical atmospheric sections have been plotted using the CCSM3 native vertical coordinate system (see online at http://www.ccsm.ucar.edu/models/atm-cam/docs/usersguide/), with sigma coordinates near the surface merging into pressure coordinates at increasing height. This avoids spurious interpolation effects encountered when converting to pressure coordinates. Hybrid and pressure coordinates are very similar away from high topography.

face heat fluxes and the shallow mixed layer depth (via wind-driven turbulence), these effects are not directly included here. Instead we focus on wind anomaly experiments wherein only ocean circulation, via Ekman transport, is directly affected. Nevertheless, the resulting SST response is similar in magnitude and distribution to the imposed (3 times standard deviation) SST perturbation used in the uncoupled experiments (see Figs. 8e,f).

The atmospheric temperature response is shown in Fig. 9. A number of important differences compared to the uncoupled experiments are immediately evident. First, away from the area directly affected by the oceanic heat anomaly, the response is generally weaker than for the uncoupled positive minus negative (P − N) or positive minus control (P − C) results. This is despite the fact that both sets of experiments have very similar ocean SST patterns and that the uncoupled positive experiment show little significant response. In the coupled experiment, a comparison between the positive and negative ensemble means with the control ensemble mean demonstrates that unlike the uncoupled experiments, there is an approximately linear response with regard to the sign of the perturbation. Figures 9b,c are almost mirror images of each other. The three different coupled comparisons show a statistically significant upper-tropospheric temperature anomaly maximum that, while at a similar height to the SAM regressed temperature response, is displaced by approximately 10° of latitude to the south. In addition, the cooling response over Antarctica that extends throughout the troposphere in the SAM regression is not seen in the perturbation response, with the experiments showing weak levels of cooling and warming poleward of 60°S. Near the surface, however, the temperature dipole directly attributable to the oceanic anomaly is of a similar magnitude and extent as that in the uncoupled experiments.

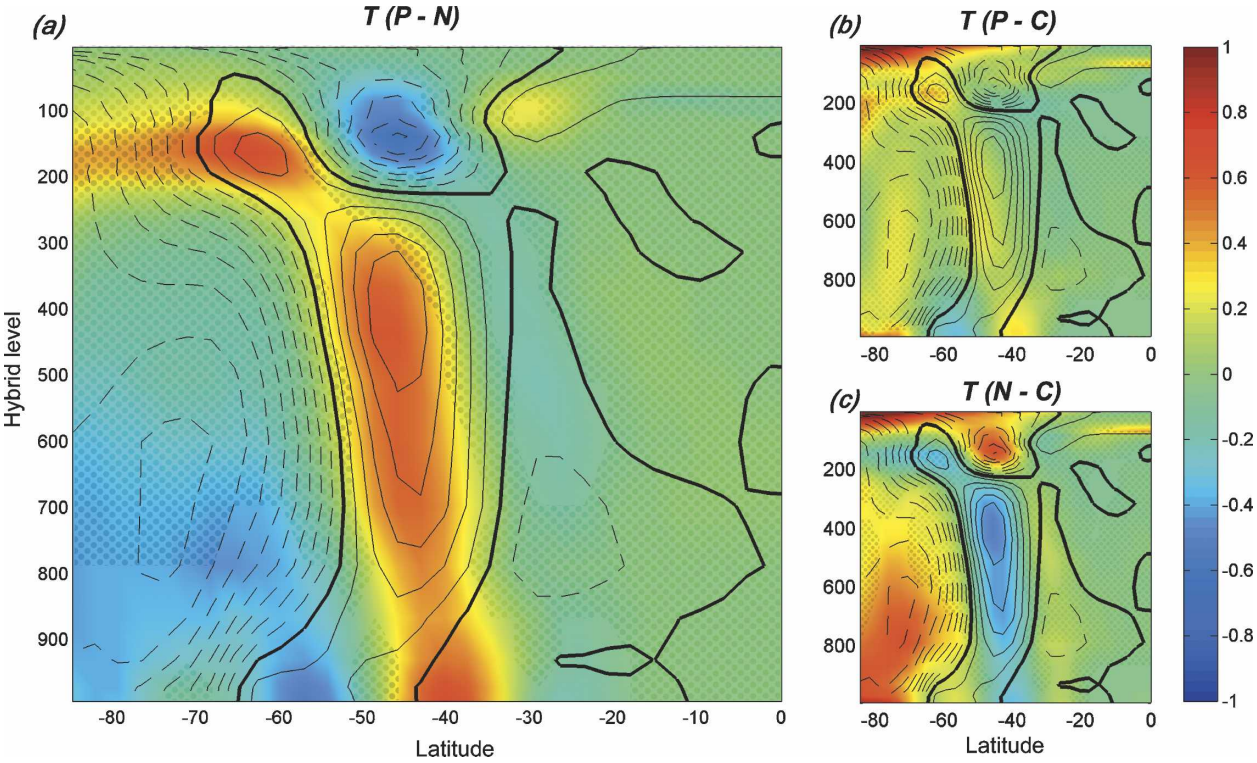

FIG. 7. Same as in Fig. 6 but for atmospheric temperature. Regression CIs are 0.1°C.

To investigate the effect of the ensemble size on the confidence that can be placed in the coupled experiment results, a Monte Carlo analysis was performed on the larger uncoupled ensemble set. Here, we randomly selected 20 ensemble members out of a possible 40 (to match the coupled ensemble size) for each of the positive and negative experiments and formed ensemble mean differences. This procedure was repeated 1000 times. The results at the height of the midlatitude temperature maximum (~400 mb) are shown in Fig. 10. While most of the cases showed a temperature maximum at a position similar to that of the regressed temperature, approximately 10% of the 1000 cases show a temperature maximum that was closer to that of the coupled experiment. In addition, where the maximum is in this more southward position (Fig. 10b), the response is on average weaker than the response associated with the more northward position consistent with the SAM regressed response (Fig. 10b). The associated full-height temperature (Figs. 10c,d) and velocity (not shown) responses also indicate that for the cases associated with the more southerly upper-tropospheric temperature maximum, there are also weak full-height temperature and zonal wind response patterns that are similar to the coupled response. This analysis demonstrates that there is a small probability that because of the smaller ensemble size, the coupled experiment response is not truly representative.

The coupled model response in the zonal and meridional wind field is shown in Fig. 11. The zonal wind response shows a distinct resemblance to the associated SAM response; however, the signal is of a considerably smaller magnitude and the upper-tropospheric minimum is shifted about 5° in latitude to the south. Only this peak is statistically significant at these altitudes. A small area at the surface, centered near 45°S, is also significant for both zonal and meridional wind components. The meridional response shows a positive anomaly in this region similar to the one clearly seen in the uncoupled positive experiment (wherein there was no evidence of a SAM-like atmospheric response). This suggests that rather than being the surface signature of the modified upper-tropospheric zonal jet (which is the case for the SAM response), the surface meridional wind is more a consequence of the direct thermal response common to all the experiments. This enhanced meridional wind is consistent with rising and falling air to the north and south, respectively, resulting from the modified SST below. An anomalous pressure gradient is then set up that, coupled with the surface drag, drives the ageostrophic meridional surface flow.

Figure 12 shows the ensemble-averaged evolution of

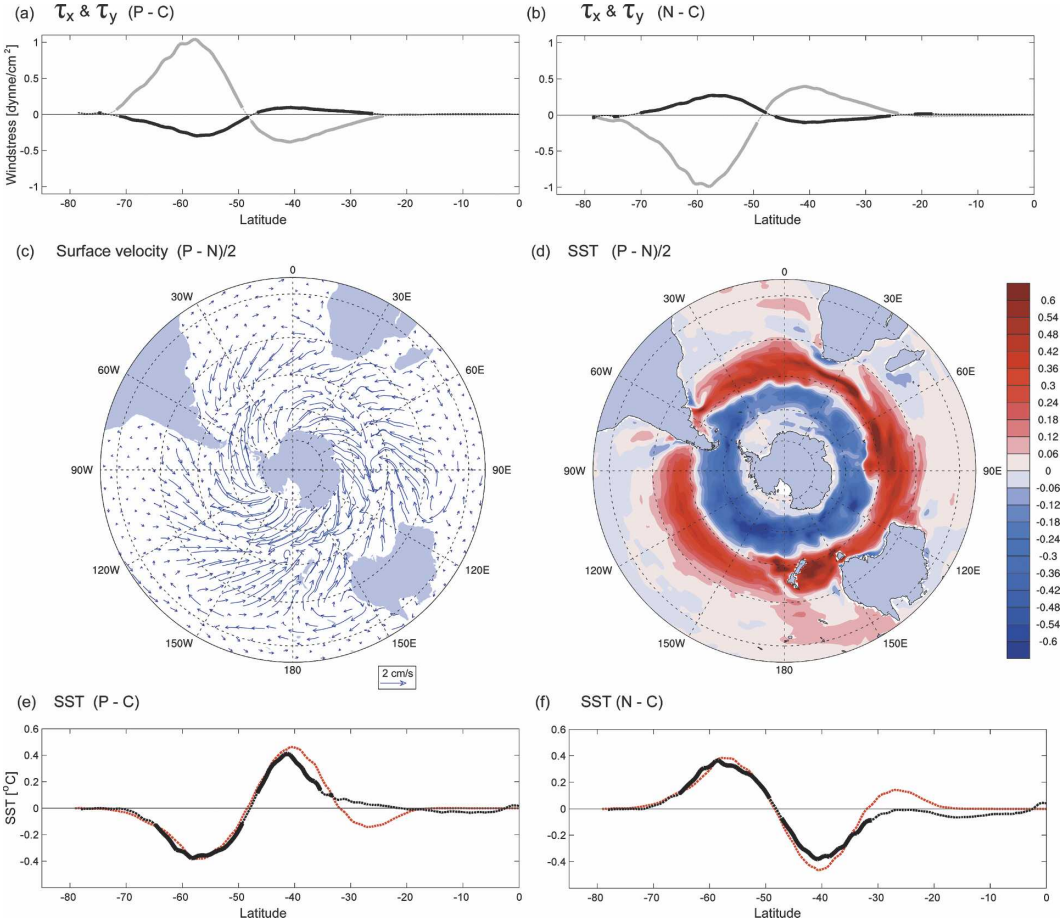

FIG. 8. Full coupled experiment results. Zonally averaged zonal (gray) and meridional (black) wind stress for (a) P − C and (b) N − C ensemble means (thick line shows a response that is significant at the 95% level with a thin dotted line otherwise). (c) Surface velocity response for P − N ensemble means (2 cm s^{-1} reference vector is shown). (d) SST response for P − N ensemble means. Responses shown in (c) and (d) are very similar to P − C and N − C responses. (e), (f) p − C and N − C zonally averaged SST, respectively. Red dotted line shows the zonally averaged SST perturbation used in the uncoupled experiments (i.e., 3 std dev SAM regressed SST).

the temperature and zonal wind over the 6 months of the coupled integrations for the positive minus negative ensemble means. The direct thermal response builds up over a period of 4–6 weeks as the SST response develops through the meridional advection of heat. There appears to be a considerable lag before the zonal wind response reaches its maximum magnitude. This is curious, as the atmosphere generally responds on short synoptic time scales. It is possible that some threshold thermal response must be reached for the nonlinear dynamics to become important and produce the enhanced upper-tropospheric response. It may, however, just be an artifact of the intrinsic variability that is still evident despite the ensemble averaging. This is probably the cause of the short-term drop in the response strength near the end of the integration. It is also possible that the atmospheric response may be sensitive to the seasonal mean-state or to the details of the time-varying wind stress perturbation. Future work will address the impact of seasonality on the atmospheric response in the Southern Annular Mode.

4. Summary and conclusions

This study aimed to identify any dynamic coupling between the ocean and atmosphere in the Southern Hemisphere extratropics. It is well established that variations at the ocean surface are due in large part to the effect of variations of temperature, humidity, and wind stress in the atmospheric boundary layer. Less well established is the nature and physics of any feedback from the ocean to the atmosphere. The deep mixed layers in the Southern Ocean and the associated high thermal storage capacity in this region suggest that

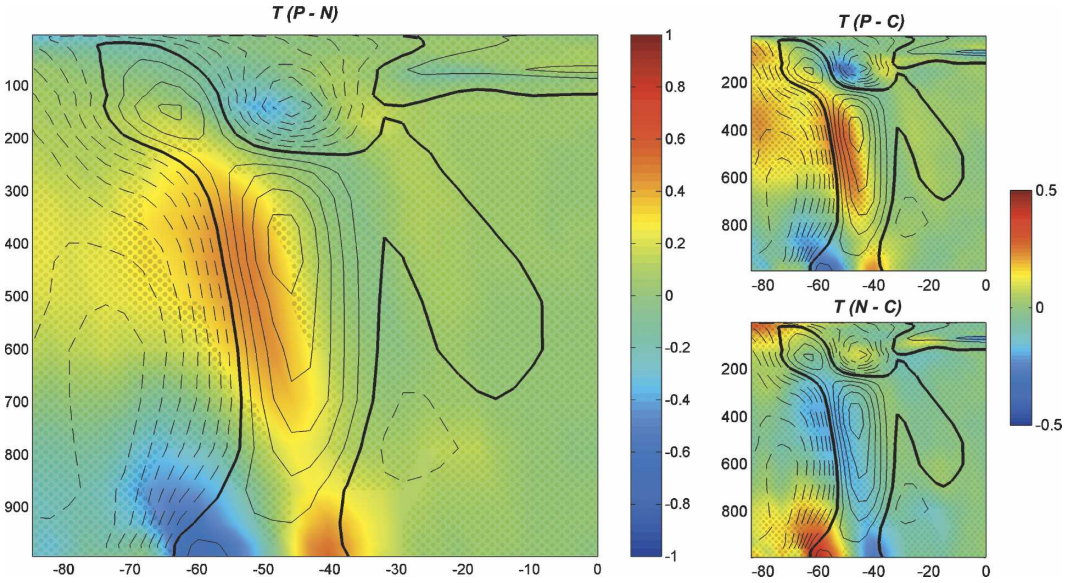

FIG. 9. (a) Difference between P and N experiment ensemble means for zonally averaged temperature (filled contours); mottling indicates areas where the difference is not significant at the 90% confidence level. Black contours show the zonally averaged temperature regressed on the SAM index (solid lines are positive, dashed lines are negative, and thick line at 0; CI is 0.1 K). (b), (c) Same as in (a) but for the difference between P vs C and N vs C ensemble means.

any ocean–atmosphere feedback could significantly extend the persistence of the driving atmospheric variability. In a review of Northern Hemisphere atmospheric responses to ocean anomalies, Kushnir et al. (2002) identified two mechanisms driving the atmospheric back interaction. First, there is a local thermodynamic interaction, wherein the ocean response to an atmospheric anomaly modifies air–sea fluxes in such a way as to reduce the damping normally experienced by the original atmospheric anomaly. The second is a nonlinear response to changes in the surface baroclinicity resulting from the modified thermal gradient, the effect of which is felt remotely and can project onto the internal modes of atmospheric variability. In the present study a comparison of uncoupled and coupled model experiments showed a significant modification in the temporal characteristics of the SAM when an ocean feedback is permitted, significantly enhancing the persistence of the coupled integration's atmospheric vacillations. To investigate the processes associated with this enhanced persistence, a set of coupled and uncoupled ensemble integrations were analyzed in which anomalous SAM-like SST patterns were imposed. In the coupled case, this was achieved via the application of a SAM-like wind stress anomaly felt only by the ocean via Ekman transport effects. While a purely dynamical perturbation is used in the coupled experiments, both the dynamically and thermodynamically forced components of the SST response to the SAM are qualitatively very similar over large parts of the extratropics (see Sen Gupta and England 2006; Figs. 8e,f). Consequently, we would expect very similar results had we applied a thermodynamic forcing.

A local thermal response is evident in all the experiments considered, producing a weak meridional temperature gradient that extends vertically to heights of ~1 km. There is an associated weak meridional wind response close to the sea surface that can be explained by anomalous rising and descending air over the regions of elevated and depressed SST. While this local response is common to all experiments after an initial development phase of a few weeks, a remote response is less consistent. The uncoupled experiments showed a nonlinear response with respect to the sign of the perturbation. This is a common feature of many of the similar Northern Hemisphere experiments undertaken by others (e.g., Kushnir et al. 2002; Deser et al. 2004; Magnusdottir et al. 2004). This nonlinearity is thought to stem from the high atmospheric sensitivity to the position of the heating, relative to the mean flow. In addition, there is an inherent nonlinearity in the depth of heating produced by the positive and negative SST anomalies associated with the modified atmospheric stability above the perturbed region. The negative SAM-like SST perturbation results in an atmospheric anomaly (in the ensemble mean) that projects strongly onto a weak negative SAM. Near the surface the SAM-like response is modified by the direct thermal re-

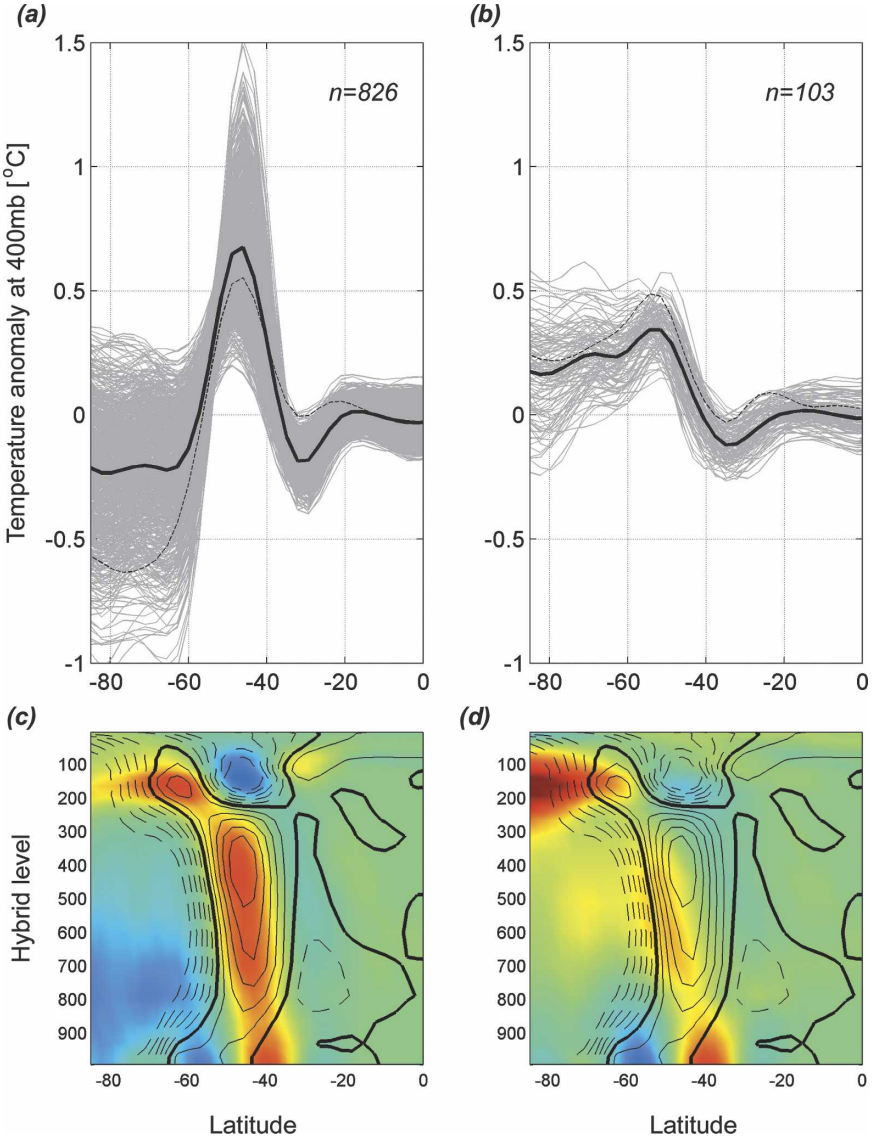

FIG. 10. Ensemble mean P − C differences of atmospheric temperature at 400 mb, for the uncoupled experiments using 1000 randomly chosen ensemble subsets, each made up of 20 of the 40 possible members (gray lines). The results are partitioned into those where the position of the temperature maximum is coincident with (a) the position of the SAM regressed temperature maximum or (b) the more southerly position of the maximum for the coupled experiment P − N response. Some of the 1000 members were discarded where their distributions did not match the required patterns. The thick black lines represent the mean of members in each of the two categories; *n* shows the number of members in each category. The dashed lines show the regression of the 400-mb temperature onto the SAM index (for the coupled experiment) in (a) and the coupled P − N perturbation response in (b). (c), (d) The mean atmospheric temperature response (and overlaid contours of SAM regression) corresponding to (a) and (b), respectively.

sponse. The positive SAM perturbation in contrast shows no significant response away from this area of direct thermal influence.

The coupled model experiments do show a linear response when the sign of the perturbation is reversed. However, the negative-phase SAM response is considerably weaker in the coupled experiments than for the negative SAM uncoupled simulations. In addition, the position of the temperature maximum (minimum) and the more northern upper-tropospheric zonal wind mini-

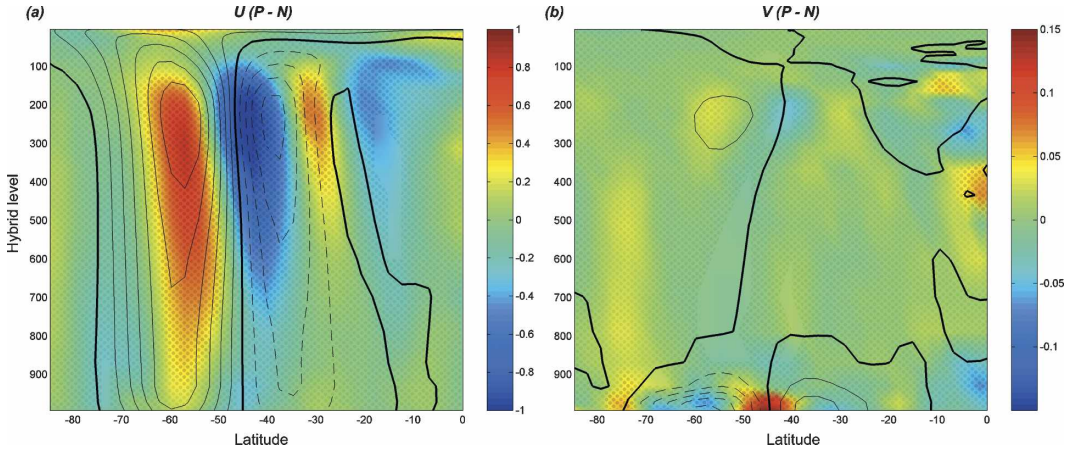

FIG. 11. Difference between P and N experiment ensemble means for zonally averaged (a) zonal and (b) meridional wind speed (filled contours); mottling indicates areas where the difference is not significant at the 90% confidence level. Black contours show the zonally averaged wind speed components regressed onto the SAM index [solid lines are positive, dashed lines are negative, and thick line at 0; CI is 0.5 m s^{-1} in (a) and 0.1 m s^{-1} in (b)].

mum (maximum) is shifted southward compared to the SAM regression for the positive (negative) perturbation. This relatively weak coupled response does not contradict the finding of enhanced SAM persistence seen in the coupled compared to uncoupled "natural variability" simulations (Fig. 4). In the case of the uncoupled ensemble experiments the addition of an SST perturbation is somewhat akin to having a dynamical response in the ocean set up by the SAM. A Monte Carlo analysis of the larger uncoupled ensemble set suggests that there is a small probability that the coupled response is unrepresentative of the true response, as a result of the smaller ensemble size. It is also important to remember that the coupled system includes a dynamic sea ice that may considerably alter the atmospheric response. For example, in the Northern Hemisphere, Magnusdottir et al. (2004) showed a strong negative feedback associated with the sea ice back interaction to the atmosphere. A further possible reason for the very different coupled and uncoupled responses may stem for the small difference in the SST perturbations (Fig. 8). In particular, the uncoupled experiments have a weak band of anomalously warm water between 20° and 30°S absent in the coupled experiments. This low-latitude anomaly may have a disproportionate effect on the response. The increased importance associated with low-latitude anomalies is noted for the SAM by Zhou and Yu (2004) and for a number of Northern Hemisphere experiments (e.g., Peng et al. 2002; Robinson et al. 2003). To test this, further atmosphere-only runs were carried out whereby the SST perturbation was modified to match the coupled experiment SST response between 20° and 30°S. The ensemble mean responses were essentially unchanged. Future work will address the sensitivity of the response to perturbations applied in different seasons.

While the simulated spatial pattern of the SAM is very similar to observations, the temporal characteristics are not as well represented. Autocorrelations of the ECMWF SAM index (not shown) demonstrate weaker persistence at a lag of one month than the various prescribed SST control runs. However, at larger lags autocorrelation levels are consistent with, or above, the coupled simulation levels. One cause for this may lie in the fact that the oceanic response to the SAM appears too strong and more zonally symmetric than observed, although like the simulation, the observed response persists for some months after the initial atmospheric SAM pattern has decayed. This is further discussed in Sen Gupta and England (2006, their Fig. 12). As a result, the initial air–sea coupling may be too strong in the model. While the ocean feedback seen in the simulation is considerably weaker than the natural atmospheric variability, the actual observed feedback may be weaker still, making its identification difficult.

Our ensemble experiments show a robust direct response to SAM-like SST perturbations that extends through the lower 1 km of the atmosphere. There is also evidence for a dynamical, indirect response that projects onto the dominant mode of atmospheric variability and extends throughout the troposphere. However, the characteristics of this response are sensitive to whether the perturbation is applied within a coupled or uncoupled simulation. This response is detectable but much weaker than the atmosphere's internal natural variability. Nevertheless, there is strong evidence to suggest that air–sea interactions do increase the persis-

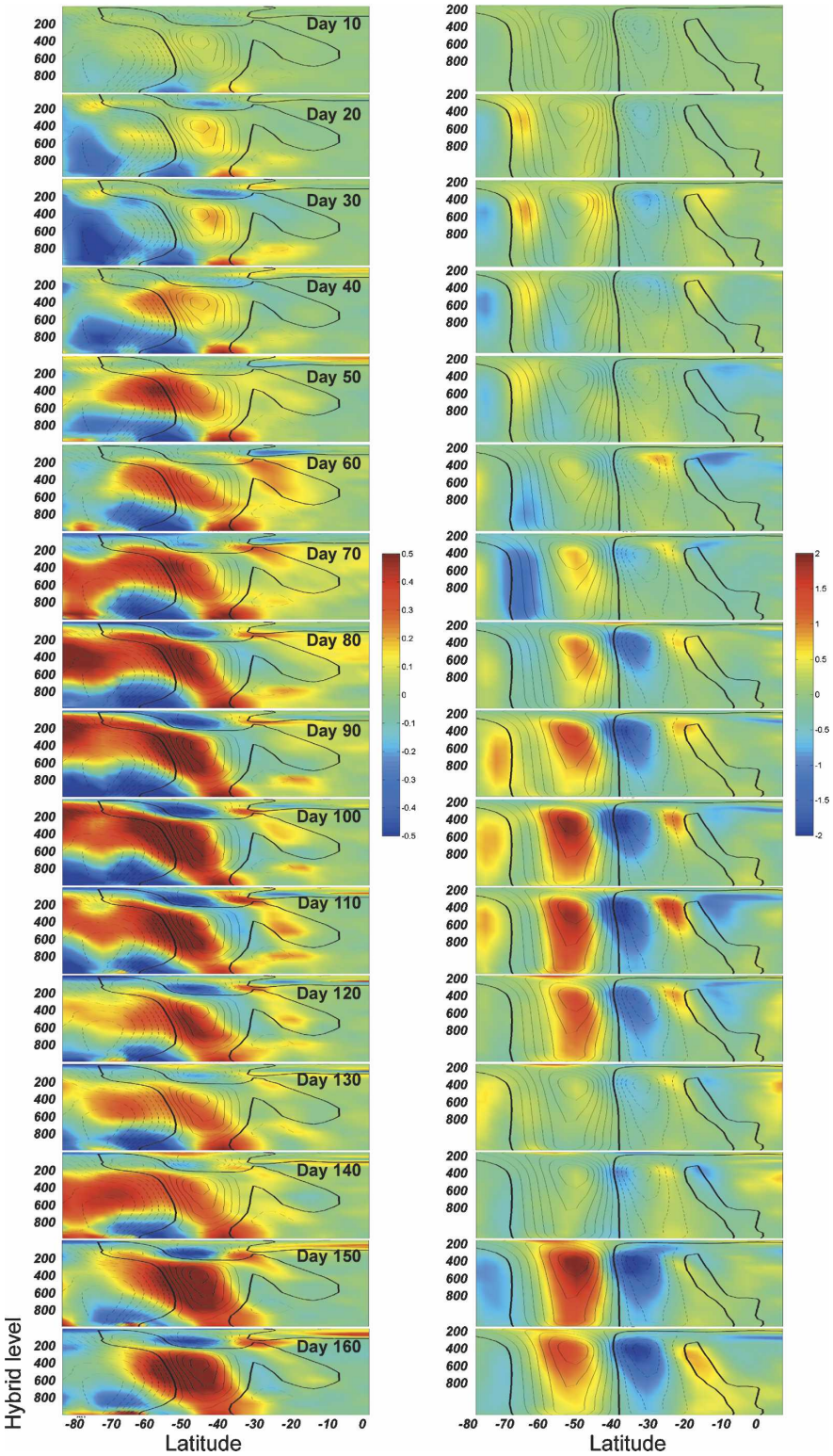

FIG. 12. Time evolution of the zonally averaged (left) temperature and (right) zonal wind ensemble mean differences for the P − N perturbation experiments. Subsequent panels are separated by 10 days and show a 20-day moving average.

tence of the SAM over interseasonal to annual time scales.

Acknowledgments. We thank the National Center for Atmospheric Research for providing the CCSM model and output datasets used in this study and the staff at the Australian Partnership for Advanced Computing (APAC) National Facility for help in setting up the model. Model experiments were run at the APAC National Facility. Correspondence with I. Watterson helped shape many aspects of the study. This project was supported by the Australian Research Council, the CSIRO Flagship Fellowship program, and the University of New South Wales International Postgraduate Research Scholarship Scheme. Finally we thank the two anonymous reviewers for their suggestions and comments.

REFERENCES

Briegleb, B. P., C. M. Bitz, E. C. Hunke, W. H. Lipscomb, M. M. Holland, J. L. Schramm, and R. E. Moritz, 2004: Scientific description of the sea ice component in the Community Climate System Model, version 3. NCAR Tech. Note NCAR/TN-463+STR, 70 pp.

Collins, W., and Coauthors, 2006a: The Community Climate System Model version 3 (CCSM3). *J. Climate,* **19,** 2122–2143.

——, and Coauthors, 2006b: The formulation and atmospheric simulation of the Community Atmosphere Model version 3 (CAM3). *J. Climate,* **19,** 2144–2161.

Danabasoglu, G., W. Large, J. Tribbia, P. Gent, B. Briegleb, and J. McWilliams, 2006: Diurnal coupling in the tropical oceans of CCSM3. *J. Climate,* **19,** 2347–2365.

Deser, C., G. Magnusdottir, R. Saravanan, and A. Phillips, 2004: The effects of North Atlantic SST and sea ice anomalies on the winter circulation in CCM3. Part II: Direct and indirect components of the response. *J. Climate,* **17,** 877–889.

Gibson, R., P. Kallberg, and S. Uppala, 1996: The ECMWF reanalysis (ERA) project. *ECMWF Newsletter,* No. 73, ECWMF, Reading, United Kingdom, 7–17.

Hall, A., and M. Visbeck, 2002: Synchronous variability in the Southern Hemisphere atmosphere, sea ice, and ocean resulting from the annular mode. *J. Climate,* **15,** 3043–3057.

Holland, M., C. M. Bitz, and E. Hunke, 2005: Mechanisms forcing an Antarctic dipole in simulated sea ice and surface ocean conditions. *J. Climate,* **18,** 2052–2066.

Kushnir, Y., W. Robinson, I. Blade, N. Hall, S. Peng, and R. Sutton, 2002: Atmospheric GCM response to extratropical SST anomalies: Synthesis and evaluation. *J. Climate,* **15,** 2233–2256.

Magnusdottir, G., C. Deser, and R. Saravanan, 2004: The effects of North Atlantic SST and sea ice anomalies on the winter circulation in CCM3. Part I: Main features and storm-track characteristics of the response. *J. Climate,* **17,** 857–876.

Oleson, K. W., and Coauthors, 2004: Technical description of the Community Land Model (CLM). NCAR Tech. Note NCAR/TN-461+STR, 174 pp.

Peng, S., W. A. Robinson, and S. Li, 2002: North Atlantic SST forcing of the NAO and relationships with intrinsic hemispheric variability. *Geophys. Res. Lett.,* **29,** 1276, doi:10.1029/2001GL014043.

Raphael, M., and M. Holland, 2006: Twentieth century simulation of the southern hemisphere climate in coupled models. Part 1: Large scale circulation variability. *Climate Dyn.,* **26,** 217–228.

Robinson, W. A., S. Li, and S. Peng, 2003: Dynamical nonlinearity in the atmospheric response to Atlantic sea surface temperature anomalies. *Geophys. Res. Lett.,* **30,** 2038, doi:10.1029/2003GL018416.

Sen Gupta, A., and M. H. England, 2006: Coupled ocean–atmosphere–ice response to variations in the Southern Annular Mode. *J. Climate,* **19,** 4457–4486.

Sutton, R., W. Norton, and S. Jewson, 2001: The North Atlantic Oscillation—What role for the ocean? *Atmos. Sci. Lett.,* **1,** 89–100.

van Loon, H., 1967: The half-yearly oscillations in middle and high southern latitudes and the coreless winter. *J. Atmos. Sci.,* **24,** 472–486.

Watterson, I. G., 2001: Zonal wind vacillation and its interaction with the ocean: Implication for interannual variability and predictability. *J. Geophys. Res.,* **106,** 965–975.

Zhou, T., and R. Yu, 2004: Sea-surface temperature induced variability of the Southern Annular Mode in an atmospheric general circulation model. *Geophys. Res. Lett.,* **31,** L24206, doi:10.1029/2004GL021473.